

Evaluation of Weather Parameters for Renewable Energy Forecasting with Echo State Networks

Samuel G. Dotson^{a,*}, Kathryn D. Huff^a

^a*Dept. of Nuclear, Plasma, and Radiological Engineering, University of Illinois at Urbana-Champaign, Urbana, IL 61801*

Abstract

Solar photovoltaic cells and wind turbines are two of the fastest growing forms of renewable energy worldwide. These sources of energy are highly variable due to their reliance on weather features such as solar irradiance and wind speed. This variability challenges the ability for grid operators to reliably meet demand through scheduling dispatchable resources. Weather and energy data from the diverse microgrid at the University of Illinois at Urbana-Champaign is used to develop accurate forecasts for total electricity demand, wind power, and solar power with echo state networks. The influence of different weather parameters on forecast accuracy are evaluated. Simulation results show that forecasts can be significantly improved by some additional predictors. These improvements are comparable to the accuracy of more sophisticated algorithms.

Keywords: renewable energy, forecasting, machine learning, echo state networks, grid planning

1. Introduction

1.1. Motivation

In response to the rising threat of climate change many countries have prioritized reducing carbon emissions. The goal set by the 2015 Paris Agreement

*Corresponding Author

Email address: sgd2@illinois.edu (Samuel G. Dotson)

5 is to prevent the global temperature from rising more than 1.5 °C above pre-
 industrial levels [1]. Virtually all current plans to reduce carbon emissions
 depend on increasing the share of energy production by renewable and clean
 energy sources, especially solar and wind [2, 3, 4, 5]. While solar and wind
 are low-carbon sources, these forms of electricity generation increase variability,
 10 which can lead to blackouts and power system failures [6]. Further, even modest
 penetrations of renewable energy negatively affect the economics of other types
 of clean energy, such as nuclear power [2, 7, 8]. This may force nuclear plants to
 shut down prematurely, at the precise moment that all clean sources of energy are
 most needed. Some existing work quantified the economic benefit of improving
 15 forecasts of renewable energy [9, 10, 11]. Improving renewable energy forecasts
 can mitigate some of the negative side effects of variability. The economic
 benefits of better forecasts include: reduced costs compared to building storage
 devices [9]; curtailment reduction and more efficient use of non-renewable sources
 [10]; and a slight, but important, amount of load-following from nuclear and
 20 biomass generators, which are unable to follow rapid changes in demand [11].
 Most proposed forecasting improvements involve new algorithms or machine
 learning techniques. However, one of the simplest approaches to improving
 forecasts is to improve the training data for such algorithms. There is a veritable
 zoo of weather parameters that can supplement target training data, but we
 25 don't know *a priori* which of these parameters will be helpful or detrimental to
 model performance. In this paper, we evaluate several common parameters for
 use in renewable energy forecasting with Echo State Networks (ESNs).

1.2. Why Echo State Networks

ESNs have several appealing features. They are simple, consisting only of a
 30 large, sparse, reservoir and a single output layer [12]; flexible and generalizable,
 while other network architectures require significant fine tuning [13]; and fast,
 due to their simple structure and few trainable weights relative to other neural
 networks. The ESN network architecture eliminates the need for complicated
 data pre-processing, such as feature extraction, that is required for other machine

35 learning and statistical algorithms [14, 15]. ESNs can also outperform other prediction techniques [16, 17, 18, 19, 20].

Classical ESNs have previously been used to forecast demand, wind energy, and solar energy [21, 17, 20]. ESNs are typically used to make extreme short term predictions, on the order of seconds or minutes [22, 23, 19], one-hour ahead
40 [18], and up to a single day ahead [21]. Forecasts must be multiple-hours to a couple of days ahead to aid unit commitment and grid-scale energy economy [9, 10, 11]. In this work we use a classic ESN architecture to forecast total demand, wind production, and solar production, 4-hours and 48-hours ahead.

There has been a lot of work to improve the forecasting capability of the basic
45 ESN. Approaches include: adding multiple reservoirs [20, 24, 25, 26], including non-linear units [27, 19], combining with other network architecture [22, 28]; and using a particle swarm approach [29, 23]. Some works mention that including weather parameters may be useful for renewable energy forecasting [30, 19], but none have demonstrated the effect each parameter has on model performance.
50 The primary goal of this work is to fill that gap.

1.3. Contributions

In this work, we use ESNs for three main prediction tasks: total electricity demand, wind energy production, and solar energy production. We split these tasks into further sub tasks, predicting 4-hours ahead and 48-hours ahead. These
55 predictions facilitate scheduling and grid planning because current market rules put renewable energy on the grid first, forcing conventional power generators to work around this variability [9]. Using ESNs to make predictions two-days ahead is unique to this paper since the longest predictions by ESNs in the literature only reach one-day ahead [21]. Finally, we repeat these tasks with several commonly
60 used weather parameters and evaluate their effect on model performance. The need to consider exogenous meteorological inputs has been noted previously. Suprisingly, sun elevation is seldom used as a correlated quantity for energy demand and wind power.

The structure of the paper is as follows: In Section 2, we discuss how data were

65 selected and processed, and we review ESNs. Section 3 shows a benchmarking exercise for our ESN implementation and presents the results. We discuss the results and future implications in Section 4.

2. Methodology

2.1. Echo State Networks

70 An ESN, sometimes called a “reservoir computer,” [31, 32, 33] is a type of recurrent neural network that replaces the many hidden layers of a conventional feed-forward neural network with a reservoir that is:

1. sparse,
2. connected by uniformly random weights, centered at zero,
- 75 3. and large (i.e. has many neurons).

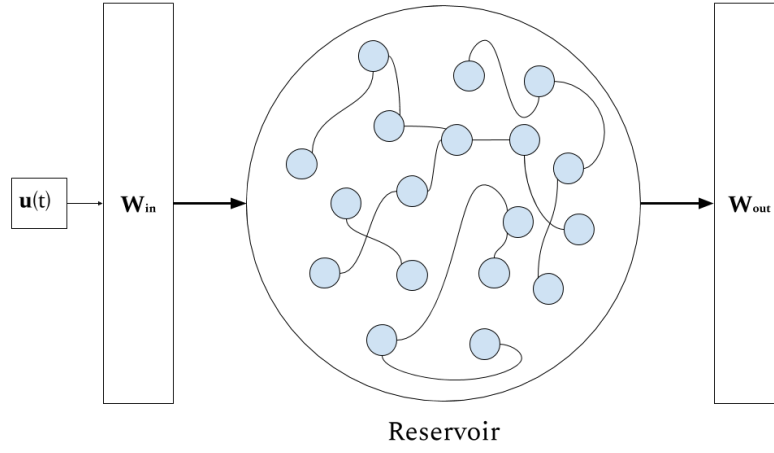
The reservoir is therefore a randomly instantiated adjacency matrix, \mathbf{W} , of size $N \times N$. The input vector, $U(t)$, of K units is mapped onto the reservoir by an input matrix, W^{in} of size $N \times K$. The activation states of the reservoir are calculated by

$$x(t) = \tanh(W^{in} \cdot U(t) + \mathbf{W}x(t-1)) \quad (1)$$

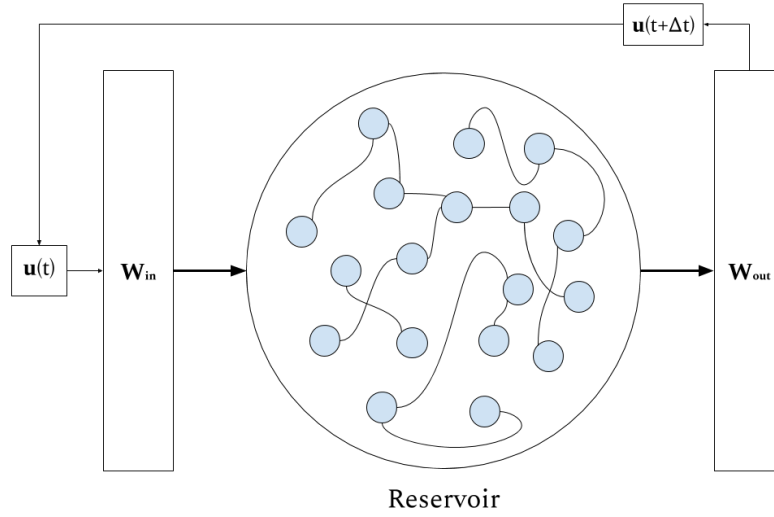
Where $x(t)$ is the collection of reservoir activations [18, 32, 12]. The output is read by an output weight matrix, W^{out} .

$$U(t + \Delta t) = (W^{out})^T \cdot x(t) \quad (2)$$

In the training phase, the output, $U(t + \Delta t)$, is discarded and the next training input is passed to the network. During the prediction phase, the output is kept and used as the next input. Figure 1 illustrates this behavior. The speed of ESNs is owed to this structure— only W^{out} has tunable weights. Everything
80 else is fixed. In this work, we adapted the open source Python package `pyESN` [34] to construct and train the network.



(a) Training Flow



(b) Predicting Flow

Figure 1: (a) Shows the behavior of an ESN during the training phase. (b) Shows ESN behavior during the predicting phase. The output $u(t + \Delta t)$ is used as the next input value.

2.2. Hyper-Parameter Optimization

ESNs are fast because the hidden layer in a conventional feed-forward neural network is replaced by a large reservoir that does not require training. The trade off is that ESNs are sensitive to various hyper-parameters that need to be optimized [12]. These hyper-parameters are summarized in Table 1. The spectral radius (ρ) should satisfy the “echo state property” which means that previous reservoir activations have a decaying influence on future states. This is usually guaranteed for $\rho < 1$, but is not a requirement [12].

Table 1: Description of Model Hyper-Parameters

Hyper-parameter	Purpose	Tested Values
noise	Neuron regularization	[0.0001, 0.0003, 0.0007, 0.001, 0.003, 0.005, 0.007, 0.01]
ρ	Spectral radius	[0.5, 0.7, 0.9, 1, 1.1, 1.2, 1.3, 1.5]
N	Size of reservoir, W	[600, 800, 1000, 1500, 2000, 2500, 3000, 4000]
sparsity	The density of connections in W	[0.005, 0.01, 0.03, 0.05, 0.1, 0.12, 0.15, 0.2]
Training Length	Size of the training set before prediction	$L \in [5000, 25000]$, step size = 300

We optimize the hyper-parameters by performing a grid search over the test values specified in Table 1. We took the following optimization steps for each prediction task:

1. Select a hyper-parameter or pair of parameters.
2. Generate ESN prediction with the specified parameters.
3. Calculate and record the root mean squared error (RMSE).
4. Continue until last entry in the parameter set is reached.
5. Set the network parameters to hyper-parameter value that minimizes the RMSE.

This algorithm generates an error surface where the coordinates of the absolute
 100 minimum correspond to the indices of values in the hyper-parameter test sets
 that minimized the RMSE. Figure 2 shows an example heatmap that optimized
 the spectral radius and noise hyperparameters for the 4-hour ahead demand
 forecast and illustrates the sensitivity of ESNs to hyperparameter values.

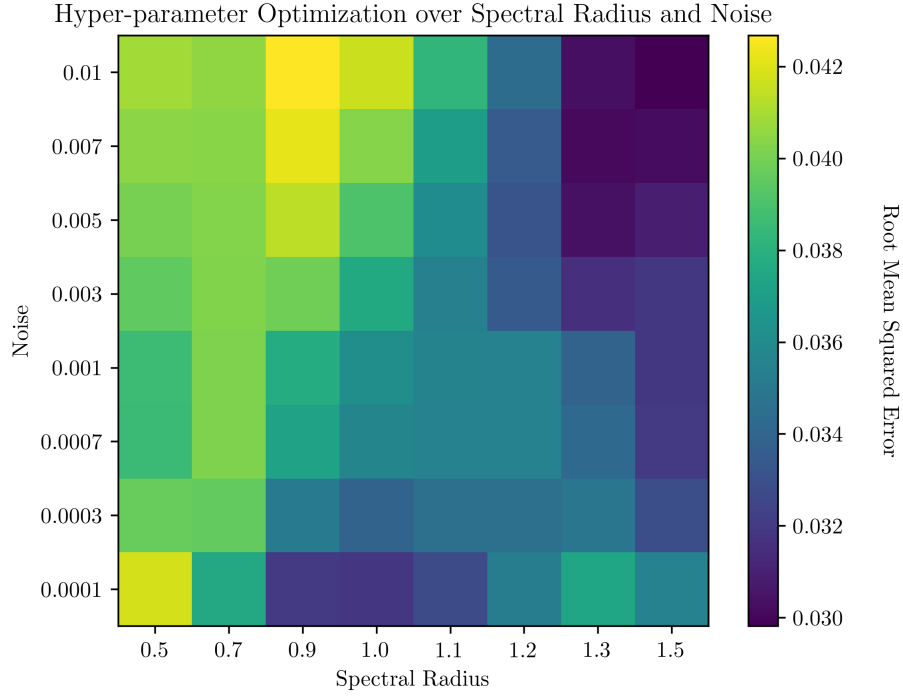


Figure 2: An example heatmap of the RMSE for 4-hour ahead demand prediction with different combinations of spectral radius, ρ , and noise.

2.3. Prediction Tasks

105 We first performed a benchmarking task by making a prediction for the
 Lorenz 1963 model [35]. Then, we optimized predictions for univariate time-
 series representing total demand, solar energy, and wind energy 4-hours ahead
 and 48-hours ahead. Finally, we repeated those same six tasks with an additional
 predictor. The tasks are summarized in Table 2.

Table 2: Summary of Prediction Tasks

Target	Future	Additional Predictor
Total Demand	4-hours ahead	None
		Solar Elevation
Solar Energy	48-hours ahead	Humidity
		Pressure
Wind Energy		Wet Bulb Temp.
		Dry Bulb Temp.
		Wind Speed

110 2.4. Data Selection and Processing

All data predicting demand, wind energy, and solar energy on the University of Illinois at Urbana-Champaign (UIUC) campus are from the UIUC Solar Farm 1.0 dashboard [36] and proprietary data shared with us courtesy of the UIUC Facilities and Services Department. All data had hourly resolution. Weather
115 data were retrieved from the National Oceanic and Atmospheric Administration (NOAA)[37] for two locations: Champaign, IL, where UIUC is located, and Lincoln, IL, where Railsplitter Windfarm is located. UIUC has a power purchase agreement with Railsplitter Windfarm [38].

In the case of UIUC solar data, significant portions were missing due to instrument failure. In order to fill in this missing data, we calculated the theoretical solar energy production based on irradiance data from OpenEI [39]. The solar output is given by [40]

$$P = G_T \eta_{ref} \tau_{pv} A [1 - \gamma (T - 25)] \text{ [W]} \quad (3)$$

where

$$G_T = P_{DNI} * \cos(\beta + \delta - lat) \quad (4)$$

$$+ P_{DHI} * \left(\frac{180 - \beta}{180} \right) \left[\frac{W}{m^2} \right]$$

where

$$\delta = 23.44 \sin \left(\left(\frac{\pi}{180} \right) \left(\frac{360}{365} \right) (N + 284) \right) [\text{degrees}] \quad (5)$$

η, τ, γ are solar panel properties

P_{DNI} is the direct normal irradiance

P_{DHI} is the diffuse horizontal irradiance

β is the tilt angle of the solar panels

The solar elevation angle, α , was also calculated [41, 42] using coordinates for the UIUC Solar Farm 1.0.

$$\alpha = \sin^{-1} [\sin(\delta) \sin(\phi) + \cos(\delta) \cos(\phi) \cos(\omega)] \quad (6)$$

where

δ is the declination angle

ϕ is the latitude of interest

ω is the hour angle

Finally, we normalized all of the data using the infinity norm

$$\|\mathbf{x}\|_{\infty} \equiv \max |x_i|. \quad (7)$$

The infinity norm is equivalent to normalizing by the system capacity. This is useful because it simplifies the comparison of our results between tasks whose training data have vastly different magnitudes. This normalization also makes it possible to compare results with other works and is consistent with the recommendation from Kobylinski et al. (2020) [43]. Table 3 gives the maximum value for each system.

Table 3: Description of the size of the UIUC microgrid

System	Maximum Value
Electricity Load	81.6 [MW]
Solar Energy	4.7 [MW]
Wind Energy	8.8 [MW]

125 2.5. Performance Metrics

We measure the accuracy of the model using two error metrics: mean absolute error (MAE) and root mean squared error (RMSE). These are defined as

$$\text{MAE} = \frac{1}{N} \sum_{i=1}^N |y_i - \hat{y}_i| \quad (8)$$

$$\text{RMSE} = \sqrt{\frac{1}{N} \sum_{i=1}^N (y_i - \hat{y}_i)^2} \quad (9)$$

where

\hat{y}_i is the predicted output

y_i is the true value

The MAE measures the expected error throughout the forecast horizon. The RMSE indicates the presence of large but infrequent errors. Since the data were normalized by system capacity [9], the error metrics are easily interpretable. In order to compare how each individual weather input changed the forecast accuracy, we calculated a “percent improvement” over the univariate case (i.e. a demand prediction based only on historical demand data). This percent improvement is calculated by

$$\% \text{ Improvement} = \frac{\hat{e} - e}{e} \times 100, [-] \quad (10)$$

where e is the error from the univariate forecast and \hat{e} is the error from the duovariate forecast. The sign indicates the direction of change in error. Finally, in order to facilitate comparison with other work, we calculated the normalized

root mean squared error (NRMSE) by

$$NRMSE = \sqrt{\frac{\sum_{i=1}^N (y_i - \hat{y}_i)^2}{\sum_{i=1}^N (y_i - \tilde{y})^2}} \quad (11)$$

where

\tilde{y} is the mean of the target set

3. Results

3.1. Benchmark: Lorenz 1963

We first verified that our choice of implementation for a conventional ESN produced similar results to those found in the literature [31]. Table 4 contains the hyper- parameters that minimized the RMSE of the model. Our optimized values differ somewhat from the literature, but our ESN implementation successfully replicated the climate of the Lorenz Attractor similar to Pathak et. al 2017. Figure 3 shows the ESN forecast ten seconds into the future for Lorenz 1963 model.

Table 4: Hyper-parameters for the Lorenz 1963 model. The random seed was generated by the open source package `numpy`.

Parameter	This paper	Literature [31]
N	2000	300
ρ	0.9	1.2
sparsity	0.1	0.1
noise	0.001	0
Training Length	3200	Not Specified
Random Seed	85	Not Specified

3.2. ESN Forecasting: Demand

We used ESNs to forecast electricity demand, or electric load, at both 4-hour intervals and 48-hour intervals. Figure 4 shows the 48-hour ahead forecast that

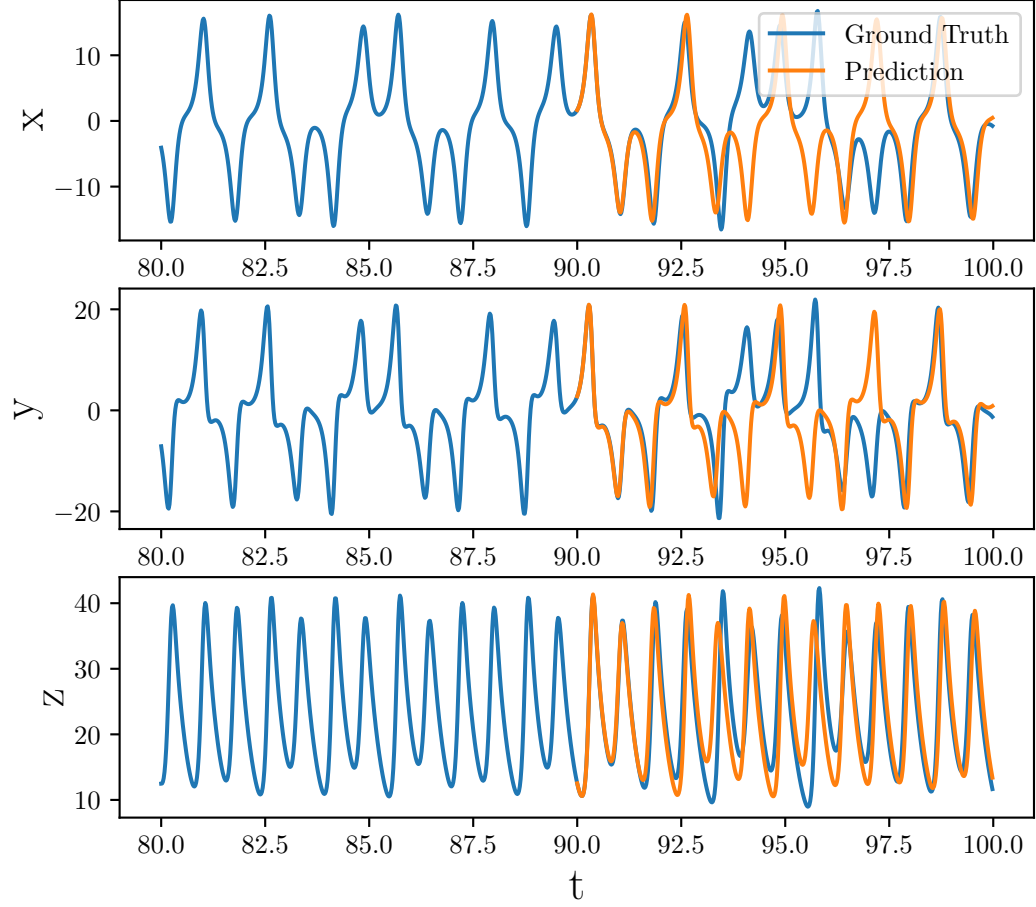


Figure 3: Using an ESN to replicate the climate of the Lorenz Attractor.

had the lowest RMSE. In this case, the forecast that used relative humidity as an additional input had the lowest error, as shown in Table 5. Table 5 also
140 shows that the forecast was weakened by training with air temperature (both wet bulb and dry bulb), air pressure, and wind speed. Adding solar elevation angle performed about the same as the base case.

Figure 5 shows the 4-hour interval forecast with the lowest RMSE. Solar elevation angle improved the forecast more than any other meteorological input.
145 Table 6 shows that humidity, air pressure, dry bulb temperature, and wind speed

worsened the forecast.

The performance of this implementation is consistent with previous applications of ESNs to the task of predicting electric load [21]. Further, these results indicate that ESNs perform better than other machine learning techniques– long short term memory (LSTM)[44], Sequence to Sequence (S2S) [44], and support
150 vector regression [15]– for predicting energy demand.

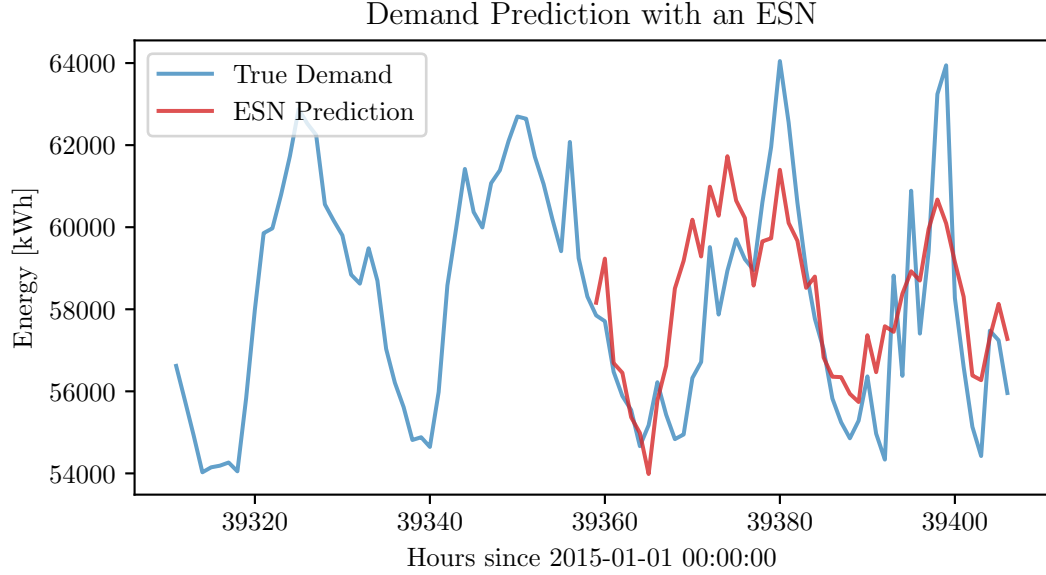


Figure 4: The optimized 48-hour ahead demand prediction. The inputs for this forecast were hourly demand and relative humidity. *Hyperparameters*: Reservoir Size: 1500, Sparsity: 0.2, Spectral Radius: 1.5, Noise: 0.0007, Training Length: 5000, Prediction Window: 48, Random state: 85

3.3. ESN Forecasting: Solar Energy

We repeated the 4-hour and 48-hour ahead forecasts for solar energy production on the UIUC campus. Figure 6 and Figure 7 show the best forecasts
155 for 48-hours ahead and 4-hours ahead, respectively. The shaded gray regions emphasize where the predicted energy production dipped below zero. This should never occur in reality. Table 7 shows that relative humidity was the best

Table 5: Tabulated error for 48-hour ahead total electricity demand forecasts with various coupled quantities. Improvement indicates the percentage improvement over the base case of forecasting electricity demand alone.

Scenario	NRMSE	MAE	RMSE	Improvement MAE (%)	Improvement RMSE (%)
Total Demand	0.76691	0.0189	0.0241	[-]	[-]
Demand + Sun Elevation	0.76351	0.0191	0.0240	+1.0582	-0.4149
Demand + Humidity	0.70799	0.0180	0.0223	-4.7619	-7.4689
Demand + Pressure	0.77769	0.0176	0.0245	-6.8783	+1.6600
Demand + Wet Bulb Temp.	0.99886	0.0241	0.0314	+27.5132	+30.2904
Demand + Dry Bulb Temp.	0.86634	0.0218	0.0273	+15.3439	+13.2780
Demand + Wind Speed	0.77958	0.0197	0.0245	+4.2328	+1.6600

additional feature for the 48-hour ahead prediction, while Table 8 shows that wet
bulb temperature improved the forecast the most. In both cases, the predictions
were improved by each feature, except for air pressure and wind speed.

Our results are comparable to other work that used ESNs to forecast solar
energy [30]. However, these results show that conventional ESNs are insufficient
for improving energy economics through day-ahead forecasting [11].

3.4. ESN Forecasting: Wind Energy

Finally, we performed the same prediction tasks as before for wind energy.
Figure 8 and Figure 9 show the best forecasts that minimized the RMSE for 48-
and 4-hours ahead, respectively. All features except air pressure improved the
forecast. Including solar elevation angle improved the 48-hour ahead forecast
the most, while adding windspeed improved the 4-hour ahead forecast the most.
Those results are shown in Table 9 and 10 respectively. Qualitatively, our
conventional ESN achieved results comparable to a more complex algorithm by
simply adding a single meteorological predictor [28]. Figure 10 shows the results
for a 48-hour ahead forecast from a complex hybrid algorithm. Chitsazan et al.
2017 compared wind speed forecasting with a conventional ESN to an ESN with

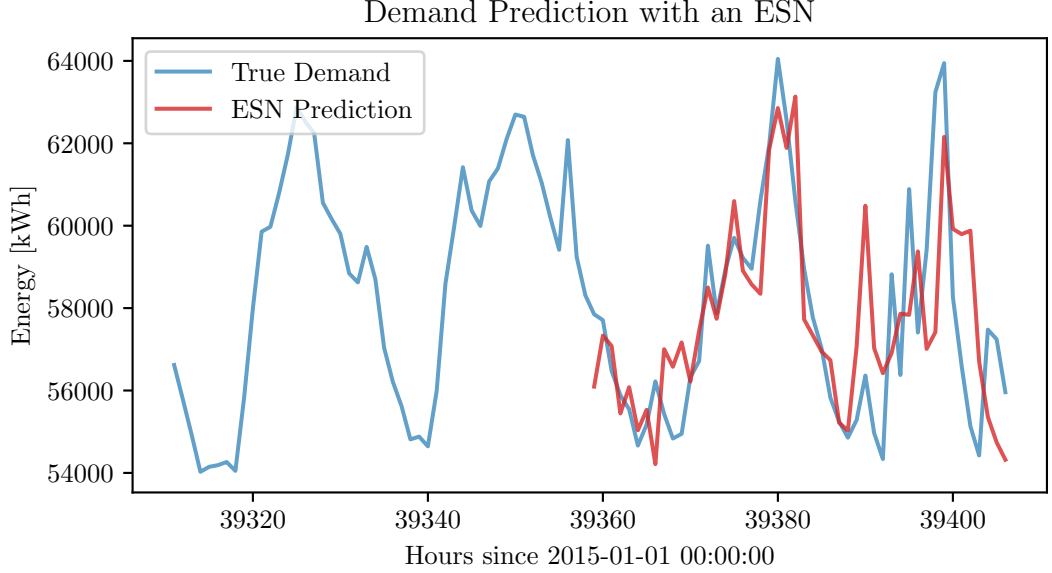


Figure 5: The optimized 4 hour ahead demand prediction. The inputs for this forecast were hourly demand and solar elevation angle. *Hyperparameters*: Reservoir Size: 2500, Sparsity: 0.01, Spectral Radius: 1.5, Noise: 0.003, Training Length: 5000, Prediction Window: 4, Random state: 85.

175 nonlinear readouts and achieved better results with the base model than we did [45]. However, this could be attributed to the fact that they used data with 10-minute resolution and 10-minute prediction steps. Unfortunately they did not include information about the hyper-parameters used for each prediction task.

Still, the state-of-the-art Weather Research and Forecasting model [46], a
 180 numerical weather prediction model, far outperforms our best results. Thus, conventional ESNs are insufficient for applications in grid planning [9].

4. Discussion

The forecast accuracy of our ESN for the Lorenz model does not persist for quite as long as in other works [31]. However, our model successfully replicates
 185 the environment that produces the Lorenz Attractor. Further, each randomly instantiated reservoir has a unique set of optimal hyper-parameters. It is

Table 6: Tabulated error for 4-hour ahead electricity demand forecasts with various coupled quantities. Improvement indicates the percentage improvement over the base case of forecasting electricity demand alone.

Scenario	NRMSE	MAE	RMSE	Improvement MAE (%)	Improvement RMSE (%)
Total Demand	0.83634	0.0193	0.0263	[-]	[-]
Demand + Sun Elevation	0.75855	0.0183	0.0239	-5.1831	-9.1255
Demand + Humidity	0.92245	0.0219	0.0290	+13.4715	+10.2662
Demand + Pressure	0.86714	0.0186	0.0273	-3.6269	+3.8023
Demand + Wet Bulb Temp.	0.80366	0.0196	0.0253	+1.5544	-3.8023
Demand + Dry Bulb Temp.	0.85662	0.0208	0.0270	+7.7720	+2.6616
Demand + Wind Speed	0.85152	0.0201	0.0268	+4.1451	+1.9011

impossible to replicate the exact conditions of other works without information about a seed for the random state. We have included this information for future work to compare with our results.

190 For each target variable— demand, wind, and solar— we found that sun elevation angle, while not always the best, was the only meteorological factor that improved the forecast error in every case. We hypothesize that the effect of additional weather features on model performance relates to the temporal complexity of that feature relative to the target variable. Electricity demand,
195 for example, is quite “predictable,” and therefore has low complexity. Air temperature and other weather related variables are less predictable. Thus, adding air temperature as a model input increases the total complexity of the system and weakens performance. Further, solar elevation angle is completely deterministic, perfectly predictable, and was the only feature that improved, or
200 neutrally effected, model performance. Like electricity demand, solar elevation angle has both diurnal and annual periodicity but has lower complexity than air temperature and electricity demand itself. Conversely, solar and wind energy are both nonlinear functions of many weather variables and consequently have

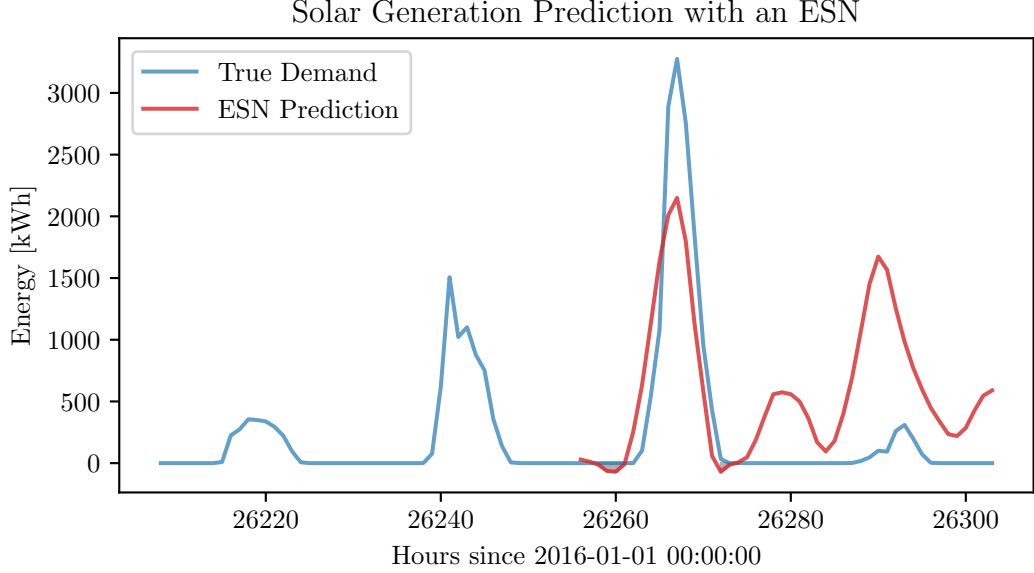


Figure 6: The optimized 48-hour ahead solar energy prediction. The inputs for this forecast were solar energy and relative humidity. Hyperparameters: Reservoir Size: 800, Sparsity: 0.2, Spectral Radius: 1.5, Noise: 0.0001, Training Length: 5000, Prediction Window: 48, Random state: 85

greater complexity than air temperature. This means that adding a temperature
 205 feature as a model input will likely decrease the total complexity of the system
 and improve the forecast. Including wind speed only improved the wind energy
 forecasts, likely because it has greater complexity than solar energy but less than
 wind energy. Relative humidity has an inconsistent and poorly understood effect
 on model performance. It improved the forecast for 48-hour ahead electricity
 210 demand but worsened it for the 4- hour ahead forecast, as shown in Table 5
 and Table 6. The opposite trend occurred for solar energy. Quantifying the
 predictability and complexity of these systems is in progress. A good measure
 for this type of complexity is the *weighted permutation entropy* [47, 48, 49].

These results point to an important disadvantage of using ESNs to forecast
 215 renewable energy: This network architecture is simple and fast, but remains
 a black box. We assume that there exists some underlying dynamics that can

Table 7: Tabulated error for 48-hour ahead solar energy forecasts with various coupled quantities. Improvement indicates the percentage improvement over the base case of forecasting solar energy alone.

Scenario	NRMSE	MAE	RMSE	Improvement MAE (%)	Improvement RMSE (%)
Solar Energy	1.27301	0.1433	0.2062	[-]	[-]
Solar + Sun Elevation	0.84908	0.0957	0.1375	-33.2170	-33.3172
Solar + Humidity	0.80107	0.1001	0.1297	-30.1465	-37.1000
Solar + Pressure	1.33226	0.1910	0.2158	+33.2868	+4.6557
Solar + Wet Bulb Temp.	1.16352	0.1519	0.1884	+6.0014	-8.6324
Solar + Dry Bulb Temp.	0.93376	0.1080	0.1512	-24.6336	-26.6731
Solar + Wind Speed	1.54306	0.2136	0.2500	+49.0579	+21.2415

be “learned,” but we cannot observe the learning process nor extract important features from ESNs.

We decided the forecast lengths based on the requirements for improved economics and planning mentioned in the literature [9, 10, 11]. The ESN model performed reasonably well at predicting 4-hours ahead but did not improve on the state-of-the-art [9, 46]. The model did not perform well at the 48-hour ahead forecasts, potentially due to the lack of higher resolution data. ESNs are known for their ability to predict highly non- linear systems [50, 51], yet using hourly data could add spurious complexity that confounds the model [48]

4.1. Future Work

One appealing avenue of continued work is to leverage ESNs to generate synthetic data that respects real dynamics. Synthetic data are often useful for other machine learning or optimization algorithms. Typically, these data are produced by sampling from an Auto-Regressive Moving Average (ARMA) model [52, 53], which tacitly assumes the training data can be made stationary. ESNs have can replicate the environment of a dynamical system, although it remains unclear how far in the future this behavior persists [31, 32]. Future work will also

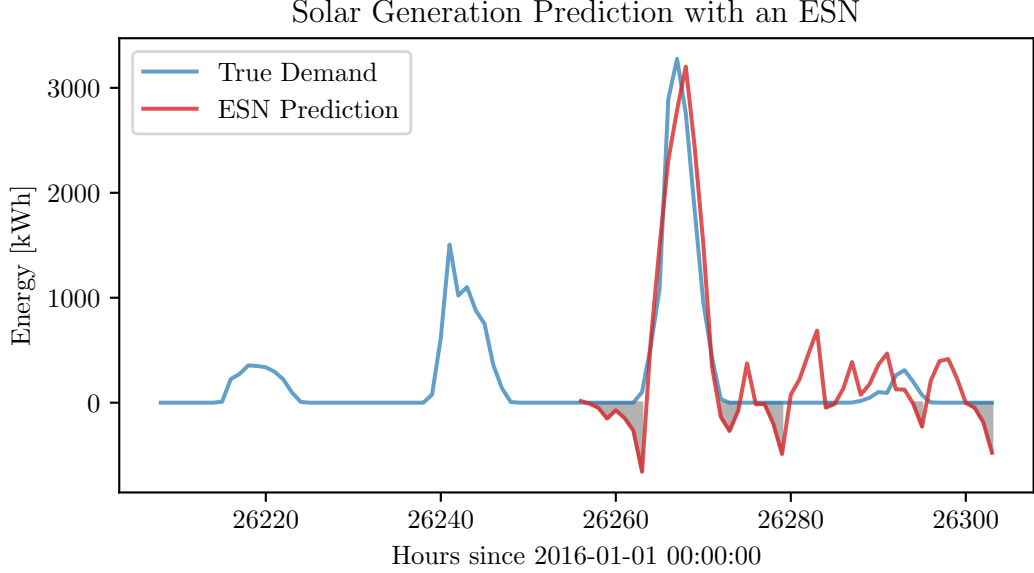


Figure 7: The optimized 4 hour ahead solar energy prediction. The inputs for this forecast were solar energy and hourly wet bulb temperature. *Hyperparameters*: Reservoir Size:800, Sparsity: 0.01, Spectral Radius: 0.9, Noise: 0.0001, Training Length: 5000, Prediction Window: 4, Random state: 85

explore the effect of data resolution on model performance, as well as evaluate
 235 some of the improvements to the ESN algorithm.

5. Conclusion

Improving renewable energy forecasting is important for grid-planning and unit commitment, especially as the share of variable renewable resources increases, challenging the baseload power from nuclear plants. We first demonstrated that
 240 our implementation of the ESN algorithm is consistent with the literature. Then, we applied this model to prediction tasks for total demand, solar energy, and wind energy, and evaluated the influence of several meteorological factors on model performance. Our results show that researchers must carefully choose each additional input to avoid increasing the system complexity. The conventional
 245 ESN used here did not demonstrate an improvement over the state-of-the-art,

Table 8: Tabulated error for 4-hour ahead solar energy forecasts with various coupled quantities. Improvement indicates the percentage improvement over the base case of forecasting solar energy alone.

Scenario	NRMSE	MAE	RMSE	Improvement MAE (%)	Improvement RMSE (%)
Solar Energy	0.59151	0.0614	0.0958	[-]	[-]
Solar + Sun Elevation	0.51383	0.0554	0.0832	-9.7720	-13.1524
Solar + Humidity	0.59943	0.0663	0.0971	+7.9804	+1.3570
Solar + Pressure	0.77968	0.0925	0.1263	+50.6515	+31.8372
Solar + Wet Bulb Temp.	0.41541	0.0526	0.0673	-14.3322	-29.7954
Solar + Dry Bulb Temp.	0.61334	0.0682	0.0993	+11.0749	+3.6534
Solar + Wind Speed	0.70216	0.0723	0.1137	+17.7524	+18.6848

nor was it accurate enough to improve grid-scale energy economy. Future work will explore other applications of ESNs and evaluate improvements to the model algorithm.

6. Acknowledgments

250 This work was made possible with the support from the people at UIUC Facilities & Services. In particular, Morgan White, Mike Marquissee, and Mike Larson. It was also aided by other members of the Advanced Reactors and Fuel Cycles (ARFC) group, in particular Nathan Ryan, Nataly Panczyk, and Gavin Davis. This work is supported by the Nuclear Regulatory Commission Fellowship
255 Program. Prof. Huff is supported by the Nuclear Regulatory Commission Faculty Development Program (award NRC-HQ-84-14-G-0054 Program B), the Blue Waters sustained-petascale computing project supported by the National Science Foundation (awards OCI-0725070 and ACI-1238993) and the state of Illinois, the DOE ARPA-E MEITNER Program (award DE-AR0000983), and the DOE
260 H2@Scale Program (Award Number: DE-EE0008832)

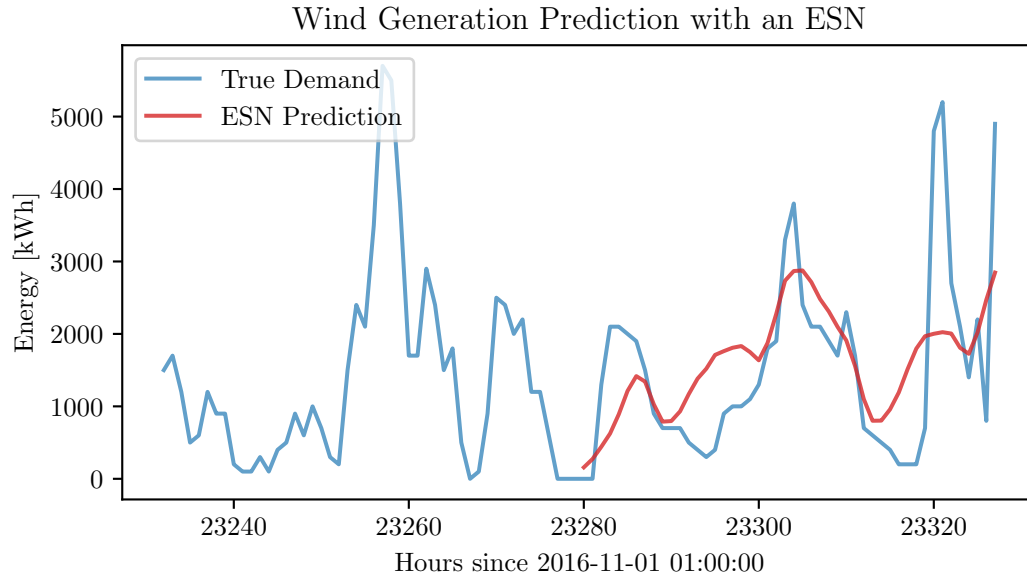


Figure 8: The optimized 48-hour ahead wind energy prediction that minimized the RMSE. The inputs for this forecast were wind energy and solar elevation angle. *Hyperparameters*: Reservoir Size:1000, Sparsity: 0.1, Spectral Radius: 0.9, Noise: 0.0001, Training Length: 19100, Prediction Window: 48, Random state: 85

References

- [1] The paris agreement | UNFCCC.
URL <https://unfccc.int/process-and-meetings/the-paris-agreement/the-paris-agreement>
- 265 [2] C. Cany, C. Mansilla, G. Mathonnière, P. da Costa, Nuclear contribution to the penetration of variable renewable energy sources in a french decarbonised power mix 150 544–555. doi:10.1016/j.energy.2018.02.122.
URL <http://www.sciencedirect.com/science/article/pii/S0360544218303566>
- 270 [3] J. Chilvers, T. J. Foxon, S. Galloway, G. P. Hammond, D. Infield, M. Leach, P. J. Pearson, N. Strachan, G. Strbac, M. Thomson, Realising transition pathways for a more electric, low-carbon energy system in the united

Table 9: Tabulated error for 48-hour ahead wind forecasts with various coupled quantities. Improvement indicates the percentage improvement over the base case of forecasting wind energy alone.

Scenario	NRMSE	MAE	RMSE	Improvement MAE (%)	Improvement RMSE (%)
Wind Energy	0.93167	0.1035	0.1308	[-]	[-]
Wind + Sun Elevation	0.81220	0.0857	0.1141	-17.1981	-12.7676
Wind + Humidity	0.84950	0.0952	0.1193	-8.0193	-8.7620
Wind + Pressure	0.98345	0.1076	0.1381	+3.9614	+5.5810
Wind + Wet Bulb Temp.	0.84323	0.0886	0.1184	-14.3961	-9.4801
Wind + Dry Bulb Temp.	0.86365	0.0815	0.1213	-21.2560	-7.2630
Wind + Wind Speed	0.84180	0.0763	0.1182	-26.2802	-9.6330

kingdom: Challenges, insights and opportunities 231 (6) 440–477, publisher: IMECHE. doi:10.1177/0957650917695448.

275 URL <https://doi.org/10.1177/0957650917695448>

[4] 99th General Assembly, Illinois general assembly - full text of SB2814.
URL [http://www.ilga.gov/legislation/fulltext.asp?DocName=
&SessionId=88&GA=99&DocTypeId=SB&DocNum=2814&GAID=13&LegID=
96125&SpecSess=&Session=](http://www.ilga.gov/legislation/fulltext.asp?DocName=&SessionId=88&GA=99&DocTypeId=SB&DocNum=2814&GAID=13&LegID=96125&SpecSess=&Session=)

280 [5] iSEE, Illinois climate action plan (iCAP).
URL [https://sustainability.illinois.edu/
campus-sustainability/icap/](https://sustainability.illinois.edu/campus-sustainability/icap/)

[6] H. Haes Alhelou, M. E. Hamedani-Golshan, T. C. Njenda, P. Siano, A survey
on power system blackout and cascading events: Research motivations and
285 challenges 12 (4) 682, number: 4 Publisher: Multidisciplinary Digital
Publishing Institute. doi:10.3390/en12040682.
URL <https://www.mdpi.com/1996-1073/12/4/682>

[7] J. H. Keppler, C. Marcantonini, O. N. E. Agency, O. for Economic Co-

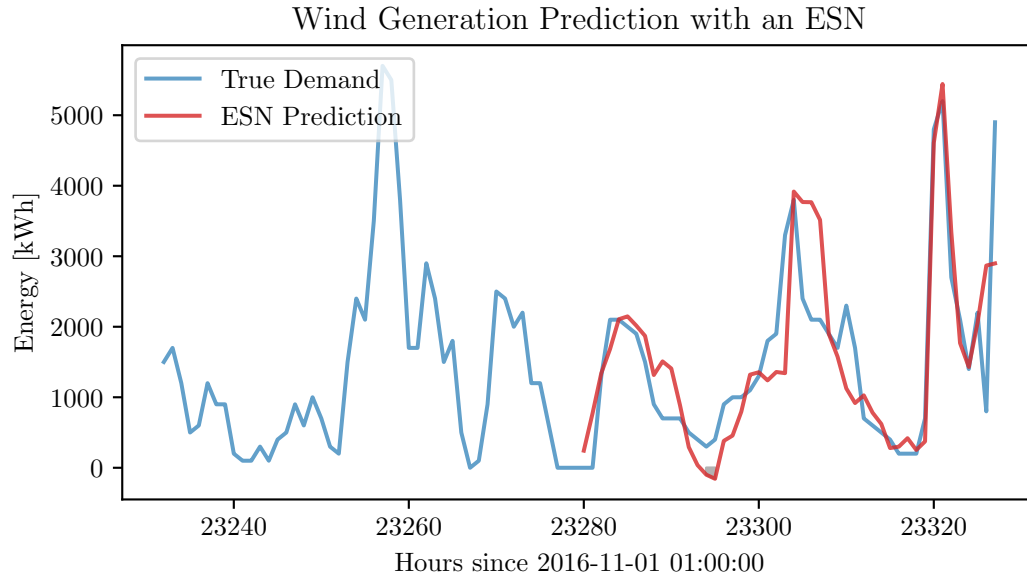


Figure 9: The optimized 4 hour ahead wind energy prediction. The inputs for this forecast were wind energy and hourly windspeed. *Hyperparameters*: Reservoir Size:1000, Sparsity: 0.15, Spectral Radius: 0.9, Noise: 0.001, Training Length: 14300, Prediction Window: 4, Random state: 85

operation {and} Development, Carbon pricing, power markets and the
 competitiveness of nuclear power, Nuclear development, Nuclear Energy
 Agency, Organisation for Economic Co-operation and Development.

- [8] Illinois Commerce Commision (ICC), I. P. A. (IPA), I. E. P. A. (IEPA),
 I. D. of Commerce and Economic Opportunity (IDCEO), Potential nuclear
 power plant closings in illinois.

URL [http://www.ilga.gov/reports/special/Report_Potential%
 20Nuclear%20Power%20Plant%20Closings%20in%20IL.pdf](http://www.ilga.gov/reports/special/Report_Potential%20Nuclear%20Power%20Plant%20Closings%20in%20IL.pdf)

- [9] Q. Wang, C. B. Martinez-Anido, H. Wu, A. R. Florita, B.-M. Hodge,
 Quantifying the economic and grid reliability impacts of improved wind
 power forecasting 7 (4) 1525–1537, conference Name: IEEE Transactions
 on Sustainable Energy. doi:10.1109/TSTE.2016.2560628.

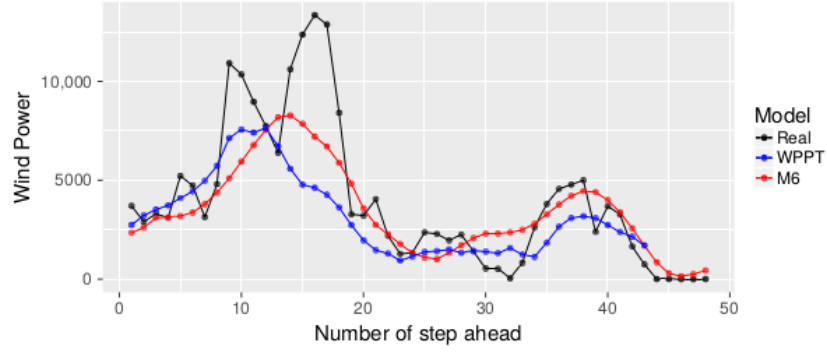


Figure 9. Forecasting using subseries $r = 1$.

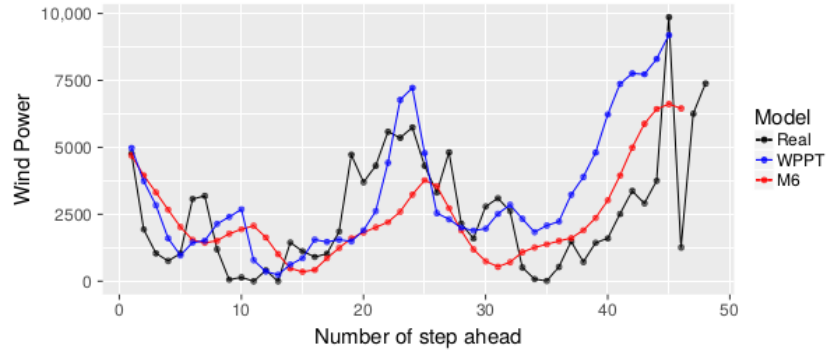
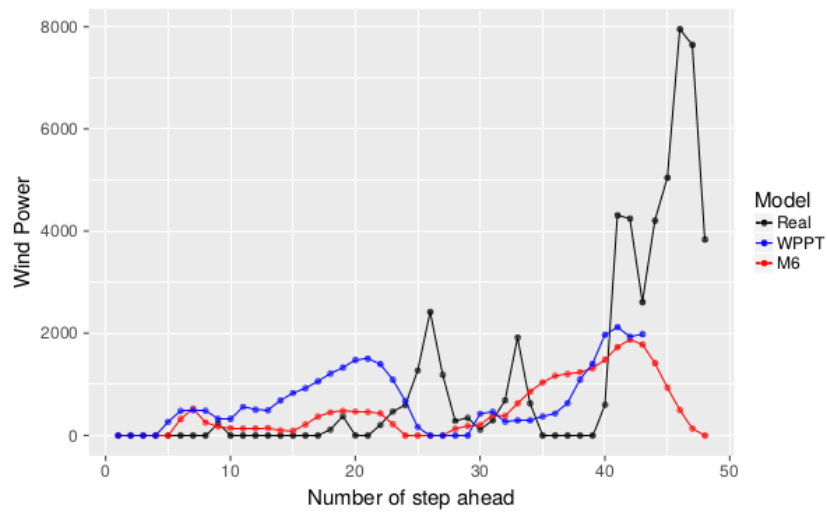


Figure 10. Forecasting using subseries $r = 5$.



24

Figure 11. Forecasting using subseries $r = 10$.

Figure 10: The results of 48-hour ahead predictions from a forecasting algorithm combining ESN and long short term memory algorithms (“M6”). Compared to the Wind Power Prediction Tool (WPPT). Figure reproduced from López et al. 2018 [28].

Table 10: Tabulated error for 4-hour ahead wind forecasts with various coupled quantities. Improvement indicates the percentage improvement over the base case of forecasting wind energy alone.

Scenario	NRMSE	MAE	RMSE	Improvement MAE (%)	Improvement RMSE (%)
Wind Energy	0.88507	0.0903	0.1243	[-]	[-]
Wind + Sun Elevation	0.83394	0.0705	0.1171	-21.9269	-5.7924
Wind + Humidity	0.85522	0.0813	0.1201	-9.9668	-3.3789
Wind + Pressure	0.88587	0.0866	0.1244	-4.0974	+0.0804
Wind + Wet Bulb Temp.	0.76203	0.0731	0.1070	-19.0476	-13.9179
Wind + Dry Bulb Temp.	0.79939	0.0747	0.1123	-17.2757	-9.9654
Wind + Wind Speed	0.59596	0.0571	0.0837	-36.7663	-32.6629

- [10] E. V. Mc Garrigle, P. G. Leahy, Quantifying the value of improved wind energy forecasts in a pool-based electricity market 80 517–524. doi:10.1016/j.renene.2015.02.023.

URL <http://www.sciencedirect.com/science/article/pii/S0960148115001135>

- [11] C. Brancucci Martinez-Anido, B. Botor, A. R. Florita, C. Draxl, S. Lu, H. F. Hamann, B.-M. Hodge, The value of day-ahead solar power forecasting improvement 129 192–203. doi:10.1016/j.solener.2016.01.049.

URL <http://www.sciencedirect.com/science/article/pii/S0038092X16000736>

- [12] M. Lukoševičius, A practical guide to applying echo state networks, in: G. Montavon, G. B. Orr, K.-R. Müller (Eds.), Neural Networks: Tricks of the Trade: Second Edition, Lecture Notes in Computer Science, Springer, pp. 659–686. doi:10.1007/978-3-642-35289-8_36.

URL https://doi.org/10.1007/978-3-642-35289-8_36

- [13] H. Liu, C. Chen, X. Lv, X. Wu, M. Liu, Deterministic wind energy

forecasting: A review of intelligent predictors and auxiliary methods 195
 328–345, publisher: Pergamon. doi:10.1016/j.enconman.2019.05.020.
 URL [http://www.sciencedirect.com/science/article/pii/](http://www.sciencedirect.com/science/article/pii/S0196890419305655)
 320 S0196890419305655

[14] D. Lazos, A. B. Sproul, M. Kay, Optimisation of energy management in
 commercial buildings with weather forecasting inputs: A review 39 587–603.
 doi:10.1016/j.rser.2014.07.053.
 URL [https://www.sciencedirect.com/science/article/pii/](https://www.sciencedirect.com/science/article/pii/S136403211400505X)
 325 S136403211400505X

[15] Y. Chen, H. Tan, U. Berardi, Day-ahead prediction of hourly electric de-
 mand in non-stationary operated commercial buildings: A clustering-based
 hybrid approach 148 228–237. doi:10.1016/j.enbuild.2017.05.003.
 URL [https://www.sciencedirect.com/science/article/pii/](https://www.sciencedirect.com/science/article/pii/S0378778816313792)
 330 S0378778816313792

[16] I. Jayawardene, G. K. Venayagamoorthy, Comparison of echo state network
 and extreme learning machine for PV power prediction, in: 2014 IEEE
 Symposium on Computational Intelligence Applications in Smart Grid
 (CIASG), pp. 1–8, ISSN: 2326-7690. doi:10.1109/CIASG.2014.7011546.

335 [17] I. Jayawardene, G. Venayagamoorthy, Comparison of adaptive neuro-fuzzy
 inference systems and echo state networks for PV power prediction 53
 92–102. doi:10.1016/j.procs.2015.07.283.

[18] G. Shi, D. Liu, Q. Wei, Energy consumption prediction of
 office buildings based on echo state networks 216 478–488.
 340 doi:10.1016/j.neucom.2016.08.004.
 URL [http://www.sciencedirect.com/science/article/pii/](http://www.sciencedirect.com/science/article/pii/S0925231216308219)
 S0925231216308219

[19] M. A. Chitsazan, M. S. Fadali, A. Tryznadlowski, Wind speed and wind
 direction forecasting using echo state network with nonlinear functions 131

- 345 879–889, publisher: Pergamon. doi:10.1016/j.renene.2018.07.060.
 URL <http://www.sciencedirect.com/science/article/pii/S0960148118308577>
- [20] H. Hu, L. Wang, S.-X. Lv, Forecasting energy consumption and
 wind power generation using deep echo state network 154 598–613.
 350 doi:10.1016/j.renene.2020.03.042.
 URL <http://www.sciencedirect.com/science/article/pii/S0960148120303645>
- [21] A. Deihimi, H. Showkati, Application of echo state networks
 in short-term electric load forecasting 39 (1) 327–340. doi:
 355 10.1016/j.energy.2012.01.007.
 URL <https://linkinghub.elsevier.com/retrieve/pii/S0360544212000126>
- [22] Y. Chen, Z. He, Z. Shang, C. Li, L. Li, M. Xu, A novel combined model
 based on echo state network for multi-step ahead wind speed forecasting: A
 360 case study of NREL 179 13–29. doi:10.1016/j.enconman.2018.10.068.
 URL <https://linkinghub.elsevier.com/retrieve/pii/S0196890418311968>
- [23] H. Wang, Z. Lei, Y. Liu, J. Peng, J. Liu, Echo state network
 based ensemble approach for wind power forecasting 201 112188.
 365 doi:10.1016/j.enconman.2019.112188.
 URL <http://www.sciencedirect.com/science/article/pii/S019689041931194X>
- [24] C. Gallicchio, A. Micheli, Deep echo state network (DeepESN): A brief
 survey [arXiv:1712.04323](https://arxiv.org/abs/1712.04323).
 370 URL <http://arxiv.org/abs/1712.04323>
- [25] X. Yao, Z. Wang, H. Zhang, A novel photovoltaic power
 forecasting model based on echo state network 325 182–189.

doi:10.1016/j.neucom.2018.10.022.

URL <http://www.sciencedirect.com/science/article/pii/S0925231218312104>

375

- [26] Q. Li, Z. Wu, R. Ling, L. Feng, K. Liu, Multi-reservoir echo state computing for solar irradiance prediction: A fast yet efficient deep learning approach 95 106481. doi:10.1016/j.asoc.2020.106481.

URL <https://linkinghub.elsevier.com/retrieve/pii/S1568494620304208>

380

- [27] G. Holzmann, H. Hauser, Echo state networks with filter and a delay&sum readout.

- [28] E. López, C. Valle, H. Allende, E. Gil, H. Madsen, Wind power forecasting based on echo state networks and long short-term memory 11 (3) 526, number: 3 Publisher: Multidisciplinary Digital Publishing Institute. doi: 10.3390/en11030526.

385

URL <https://www.mdpi.com/1996-1073/11/3/526>

- [29] N. Chouikhi, B. Ammar, N. Rokbani, A. M. Alimi, PSO-based analysis of echo state network parameters for time series forecasting 55 211–225. doi:10.1016/j.asoc.2017.01.049.

390

URL <https://linkinghub.elsevier.com/retrieve/pii/S1568494617300649>

- [30] Q. Li, Z. Wu, R. Ling, M. Tan, Echo state network-based spatio-temporal model for solar irradiance estimation 158 3808–3813, publisher: Elsevier. doi:10.1016/j.egypro.2019.01.868.

395

URL <http://www.sciencedirect.com/science/article/pii/S1876610219309105>

- [31] J. Pathak, Z. Lu, B. R. Hunt, M. Girvan, E. Ott, Using machine learning to replicate chaotic attractors and calculate lyapunov exponents from data 27 (12) 121102. arXiv:1710.07313, doi:10.1063/1.5010300.

400

URL <http://arxiv.org/abs/1710.07313>

- [32] J. Pathak, B. Hunt, M. Girvan, Z. Lu, E. Ott, Model-free prediction of large spatiotemporally chaotic systems from data: A reservoir computing approach 120 (2) 024102, publisher: American Physical Society. doi: 10.1103/PhysRevLett.120.024102.
 URL <https://link.aps.org/doi/10.1103/PhysRevLett.120.024102>
- [33] P. R. Vlachas, J. Pathak, B. R. Hunt, T. P. Sapsis, M. Girvan, E. Ott, P. Koumoutsakos, Backpropagation algorithms and reservoir computing in recurrent neural networks for the forecasting of complex spatiotemporal dynamics 126 191–217. doi:10.1016/j.neunet.2020.02.016.
 URL <http://www.sciencedirect.com/science/article/pii/S0893608020300708>
- [34] C. Korndörfer, pyESN.
 URL <https://github.com/cknd/pyESN>
- [35] E. N. Lorenz, Deterministic nonperiodic flow 20 (2) 130–141, publisher: American Meteorological Society Section: Journal of the Atmospheric Sciences. doi:10.1175/1520-0469(1963)020<0130:DNF>2.0.CO;2.
 URL https://journals.ametsoc.org/view/journals/atsc/20/2/1520-0469_1963_020_0130_dnf_2_0_co_2.xml
- [36] AlsoEnergy, University of illinois solar farm dashboard,
<http://go.illinois.edu/solar>.
 URL <http://go.illinois.edu/solar>
- [37] N. C. for Environmental Information, Find a station | data tools | climate data online (CDO) | national climatic data center (NCDC).
 URL <https://www.ncdc.noaa.gov/cdo-web/datatools/findstation>
- [38] S. Breitweiser, Wind power: University of illinois at urbana-champaign.
 URL https://www.fs.illinois.edu/docs/default-source/news-docs/newsrelease_windppa___factsheet.pdf?sfvrsn=43aaffea_0

- 430 [39] National solar radiation data base - NSRDB viewer - OpenEI datasets.
 URL [https://openei.org/datasets/dataset/
 national-solar-radiation-data-base/resource/
 b2074dd9-36a4-4382-a12f-e795b578404c](https://openei.org/datasets/dataset/national-solar-radiation-data-base/resource/b2074dd9-36a4-4382-a12f-e795b578404c)
- [40] H. E. Garcia, J. Chen, J. S. Kim, M. G. McKellar, W. R. Deason,
 435 R. B. Vilim, S. M. Bragg-Sitton, R. D. Boardman, Nuclear hybrid
 energy systems regional studies: West texas & northeastern arizona.
 doi:10.2172/1236837.
 URL <https://www.osti.gov/biblio/1236837-nuclear-hybrid-energy-systems-regional-studies->
- [41] N. US Department of Commerce, ESRL global monitoring laboratory -
 440 global radiation and aerosols.
 URL [https://www.esrl.noaa.gov/gmd/grad/solcalc/calcdetails.
 html](https://www.esrl.noaa.gov/gmd/grad/solcalc/calcdetails.html)
- [42] J. Meeus, Astronomical Algorithms, 2nd Edition, Willmann-Bell, Inc.
- [43] P. Kobylinski, M. Wierzbowski, K. Piotrowski, High-resolution net load
 445 forecasting for micro-neighbourhoods with high penetration of renewable
 energy sources 117 105635. doi:10.1016/j.ijepes.2019.105635.
 URL [http://www.sciencedirect.com/science/article/pii/
 S0142061518335257](http://www.sciencedirect.com/science/article/pii/S0142061518335257)
- [44] D. L. Marino, K. Amarasinghe, M. Manic, Building energy load forecasting
 450 using deep neural networks, in: IECON 2016 - 42nd Annual Conference
 of the IEEE Industrial Electronics Society, pp. 7046–7051. doi:10.1109/
 IECON.2016.7793413.
- [45] M. A. Chitsazan, M. S. Fadali, A. K. Nelson, A. M. Trzynadlowski, Wind
 speed forecasting using an echo state network with nonlinear output func-
 455 tions, in: 2017 American Control Conference (ACC), pp. 5306–5311, ISSN:
 2378-5861. doi:10.23919/ACC.2017.7963779.

- [46] J. G. Powers, J. B. Klemp, W. C. Skamarock, C. A. Davis, J. Dudhia, D. O. Gill, J. L. Coen, D. J. Gochis, R. Ahmadov, S. E. Peckham, G. A. Grell, J. Michalakes, S. Trahan, S. G. Benjamin, C. R. Alexander, G. J. Dimego, W. Wang, C. S. Schwartz, G. S. Romine, Z. Liu, C. Snyder, F. Chen, M. J. Barlage, W. Yu, M. G. Duda, The weather research and forecasting model: Overview, system efforts, and future directions 98 (8) 1717–1737, publisher: American Meteorological Society Section: Bulletin of the American Meteorological Society. doi:10.1175/BAMS-D-15-00308.1. URL <https://journals.ametsoc.org/view/journals/bams/98/8/bams-d-15-00308.1.xml>
- [47] B. Fadlallah, B. Chen, A. Keil, J. Príncipe, Weighted-permutation entropy: A complexity measure for time series incorporating amplitude information 87 (2) 022911, publisher: American Physical Society. doi:10.1103/PhysRevE.87.022911. URL <https://link.aps.org/doi/10.1103/PhysRevE.87.022911>
- [48] J. Garland, R. James, E. Bradley, Model-free quantification of time-series predictability 90 (5) 052910, publisher: American Physical Society. doi:10.1103/PhysRevE.90.052910. URL <https://link.aps.org/doi/10.1103/PhysRevE.90.052910>
- [49] F. Pennekamp, A. C. Iles, J. Garland, G. Brennan, U. Brose, U. Gaedke, U. Jacob, P. Kratina, B. Matthews, S. Munch, M. Novak, G. M. Palamara, B. C. Rall, B. Rosenbaum, A. Tabi, C. Ward, R. Williams, H. Ye, O. L. Petchey, The intrinsic predictability of ecological time series and its potential to guide forecasting 89 (2) e01359, _eprint: <https://esajournals.onlinelibrary.wiley.com/doi/pdf/10.1002/ecm.1359>. doi:<https://doi.org/10.1002/ecm.1359>. URL <https://esajournals.onlinelibrary.wiley.com/doi/abs/10.1002/ecm.1359>
- [50] H. Jaeger, Harnessing nonlinearity: Predicting chaotic systems

and saving energy in wireless communication 304 (5667) 78–80.
doi:10.1126/science.1091277.
URL <https://www.sciencemag.org/lookup/doi/10.1126/science.1091277>

490 [51] M. Lukoševičius, H. Jaeger, Reservoir computing approaches
to recurrent neural network training 3 (3) 127–149. doi:
10.1016/j.cosrev.2009.03.005.
URL <http://www.sciencedirect.com/science/article/pii/S1574013709000173>

495 [52] T. E. Baker, A. S. Epiney, C. Rabiti, E. Shittu, Optimal sizing of flexible
nuclear hybrid energy system components considering wind volatility 212
498–508.

[53] H. E. Garcia, J. Chen, J. S. Kim, R. B. Vilim, W. R. Binder, S. M.
Bragg Sitton, R. D. Boardman, M. G. McKellar, C. J. J. Paredis, Dynamic
500 performance analysis of two regional nuclear hybrid energy systems 107
234–258. doi:10.1016/j.energy.2016.03.128.
URL <http://www.sciencedirect.com/science/article/pii/S0360544216303759>